

Development Length of Headed Bar Based on Nonuniform Bond Stress Distribution

by Hyeon-Jong Hwang, Hong-Gun Park, and Wei-Jian Yi

The anchorage capacity of headed bars shows large variations according to design conditions, such as diameter of reinforcing bars, location of anchorage, and the use of fiber-reinforced concrete. In the present study, a design method was studied considering such various design conditions. In the proposed model, the anchorage strength of a headed bar was defined as the sum of the contributions of the straight bar length and the head bearing. Particularly, a nonuniform bond stress distribution model was used for the straight bar length. The proposed method was applied to 361 existing test specimens with various conditions of headed bar anchorage, including compression-compression-tension (CCT) node, lap splice, and beam-column joint. The predicted results were compared to the existing test results and the predictions of current design codes including ACI 318 and Model Code 2010. The results showed that the proposed model predicted the test results with reasonable precision.

Keywords: bearing force; bond strength; bond test; development length; headed bar.

INTRODUCTION

Generally, development lengths of headed bars are shorter than those of straight bars or hooked bars. For better constructability and cost saving, headed bars are usually used under various design conditions, including ends of flexural members, compression-compression-tension (CCT) node, lap splice, beam-column joint, and transverse reinforcement. The use of headed bars is particularly preferred in beam-column joints and structures with large-diameter bars such as nuclear power plants to reduce reinforcing bar congestions. Recently, the use of headed bars for new materials such as fiber-reinforced concrete, ultra-high-performance concrete (UHPC), high-strength reinforcing bars, and large-diameter reinforcing bars has been increasing.

Current design codes, including ACI 318-14¹ and Model Code 2010,² specify headed bar development lengths. To evaluate the anchorage strength of headed bars under various design conditions, CCT node test, beam end test, splice test, and beam-column joint test should be performed (refer to Fig. 1). However, the number of test results for headed bars is currently limited. For this reason, current design codes define the design equation for headed bar development length based on that of hooked bars with relatively limited applications. Further, current design codes limit the application range of the design equations, considering the material properties, minimum concrete cover, head size, and spacing of headed bars. Thus, to use headed bars in various design conditions, the development length of headed bars needs to be accurately evaluated and a large number of test results are required to verify the effect of new design parameters. From

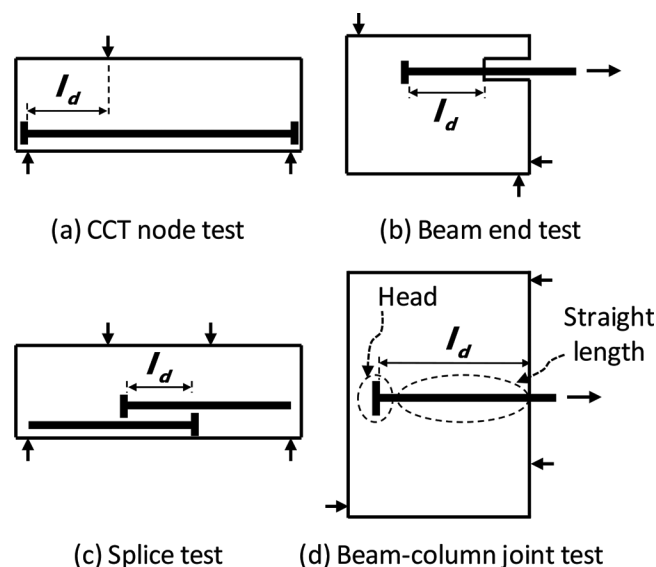


Fig. 1—Test methods for headed bar bond strength.

this viewpoint, theoretical studies are needed to develop a rational design method or guide the direction of future experimental and theoretical studies.

Various studies have been performed to evaluate the development length of headed bars. Bashandy³ tested 32 beam-column joint specimens of two headed bars with/without transverse reinforcement and reported that the headed bar strength was affected by both bond strength and head bearing strength. Wright and McCabe⁴ tested 70 beam end specimens with straight, hooked, or headed bars. The results showed that the anchorage behavior of the headed bar was similar to that of the hooked bars while the development length of the headed bars was less than that of the hooked bars. Choi et al.⁵ and Choi⁶ reported that the pullout behavior of headed bars with embedment lengths less than $15d_b$ was similar to that of 90-degree hooked bars. The pullout strength of headed bars was affected by transverse reinforcement and spacing of headed bars. Thompson et al.⁷⁻¹⁰ performed 42 CCT node tests with a headed bar and 19 lap splice tests using six headed bars, and proposed a design equation addressing the contributions of straight development length and head bearing. The test results were adopted to develop

ACI Structural Journal, V. 116, No. 2, March 2019.

MS No. S-2017-322.R2, doi: 10.14359/51712274, was received April 15, 2018, and reviewed under Institute publication policies. Copyright © 2019, American Concrete Institute. All rights reserved, including the making of copies unless permission is obtained from the copyright proprietors. Pertinent discussion including author's closure, if any, will be published ten months from this journal's date if the discussion is received within four months of the paper's print publication.

a design equation for headed bars in ACI 318.¹ Hong et al.¹¹ tested 12 beam-column joint specimens of a headed bar without transverse reinforcement showing joint shear failure and proposed a strut-and-tie model to predict the development length. Chun¹² tested 24 lap splice specimens with four headed bars to investigate the effects of high-strength bars and small side concrete cover of $1d_b$ on bond strength of the headed bars. Chun et al.¹³ tested 27 beam-column joint specimens using two headed bars with a large bar diameter of $d_b = 43.0$ and 57.3 mm (1.7 and 2.3 in.), side concrete cover of $1d_b$, and transverse reinforcement. They proposed an empirical equation for headed bar development length in beam-column joints. Sim et al.¹⁴ tested 20 beam-column joint specimens using two headed bars and steel fiber-reinforced UHPC with $f'_c = 130$ and 226 MPa (18.9 and 32.8 ksi), and reported that headed bars were yielded even with short development length of $4d_b$. Shao et al.¹⁵ tested 202 beam-column joint specimens, 10 CCT node specimens, and six splice specimens and proposed an empirical equation for development length considering the effects of transverse reinforcement, concrete cover, and spacing of headed bars. In ACI 318-14,¹ the development length of a headed bar is defined as 0.8 times that of a hooked bar. However, the effects of concrete thickness and transverse bars are not considered. In Model Code 2010,² the yield strength of a headed bar can be developed by: 1) the head anchorage only; or 2) a combination of the head anchorage and bond strength along the reinforcing bar length. Considering the average bond strength, a design equation for development length of hooked bar is applied to the design of headed bar.

Recently, Hwang et al.^{16,17} developed a nonuniform bond stress distribution model for the development length of straight reinforcing bars and hooked reinforcing bars, considering the variation in bar bond strength along the development length and hook anchorage. When the relative displacement between the reinforcing bar and concrete increases, local bond failure can occur, causing nonuniform bond stress distribution along the development length.

In the present study, the existing nonuniform bond stress distribution model proposed by Hwang et al.^{16,17} was modified to derive a unified design equation for the headed bar development length under various design conditions, including CCT node, lap splice, and beam-column joint. To verify the validity of the proposed method, the method was applied to existing headed bar test specimens. The predictions were then compared to test results.

RESEARCH SIGNIFICANCE

Unlike existing empirical design equations and methods, the proposed model is based on theoretical backgrounds of nonuniform bond stress distribution of straight bar length and concrete failure mode of head bearing. Further, the proposed method is applicable to various design conditions, covering broad ranges of design parameters (headed bar diameter $d_b = 15.9$ to 57.3 mm [0.6 to 2.3 in.], net head area-to-reinforcing bar area $A_{nh}/A_b = 1.1$ to 14.9 , concrete strength $f'_c = 20.3$ to 226.0 MPa [2.9 to 32.8 ksi], and yield strength of the reinforcing bar $f_y = 433$ to 959 MPa [62.8 to 139.1 ksi] in CCT node, lap splice, and beam-column joint

test specimens). Thus, the proposed model provides novel insight into the development of new design equations and future experimental and theoretical studies.

EXISTING DESIGN METHODS

ACI 318-14¹ permits the use of headed bars satisfying Class HA heads specified in ASTM A970¹⁸ as follows:

1. The bearing face of a headed bar should be flat face and perpendicular to the longitudinal axis of the reinforcing bar.
2. The minimum net head bearing area, which is the gross area of the head minus the cross-sectional area of the reinforcing bar, should be at least four times the nominal cross-sectional area of the reinforcing bar (that is, $A_{nh} \geq 4A_b$).
3. The length and diameter of interruptions for connection between the reinforcing bar and bearing face should not be greater than $2d_b$ and $1.5d_b$, respectively.
4. The bearing force of the head should be greater than the minimum specified tensile strength of the reinforcing bar.

In ACI 318-14,¹ Model Code 2010,² Thompson et al.,¹⁰ and Shao et al.,¹⁵ the development length l_d of headed bars is defined as a function of reinforcing bar diameter, reinforcing bar yield strength, and concrete compressive strength. Additionally, the effects of concrete cover, bar spacing, transverse reinforcement, and head bearing force are considered (Fig. 2).

In ACI 318-14,¹ the development length of a headed bar is defined as follows

$$l_d = \frac{0.19f_y d_b \psi_e}{\sqrt{f'_c}} \geq 8d_b \text{ and } 152.4 \text{ mm (in MPa and mm)} \quad (1)$$

where f_y is yield strength of the headed bar; d_b is reinforcing bar diameter; f'_c is concrete compressive strength; and ψ_e is coefficient of epoxy-coated bars ($= 1.0$ to 1.2). Unlike the development length of hooked bars, the effects of concrete cover, confining bar, and concrete type on the development length are not considered. Instead, the use of Eq. (1) is limited to the following design conditions: f_y less than 414 MPa (60 ksi), d_b less than 35.8 mm (1.4 in.), normal-weight concrete, clear cover thickness of at least $2d_b$, and clear spacing between reinforcing bars of at least $4d_b$.

In Model Code 2010,² the basic development length of a headed bar is specified to be the same to that of a hooked bar

$$l_d = \frac{(f_y - 60f_{mbd})d_b}{4f_{mbd}} \geq l_{m0} \text{ (in MPa and mm)} \quad (2a)$$

$$f_{mbd} = (\alpha_{m2} + \alpha_{m3})f_{bd0} < 2.5f_{bd0} < \sqrt{f'_c} \text{ (in MPa)} \quad (2b)$$

$$f_{bd0} = 0.35\eta_3\eta_4\sqrt{f'_c} \text{ (in MPa and mm)} \quad (2c)$$

$$\alpha_{m2} = \sqrt{(c_d/d_b)(c_m/c_d)^{0.15}} \quad (2d)$$

$$\alpha_{m3} = k_d(K_{mtr} - \alpha_t/50) \geq 0 \quad (2e)$$

$$K_{mtr} = \sum A_{tr}/(s_n d_b) \leq 0.05 \quad (2f)$$

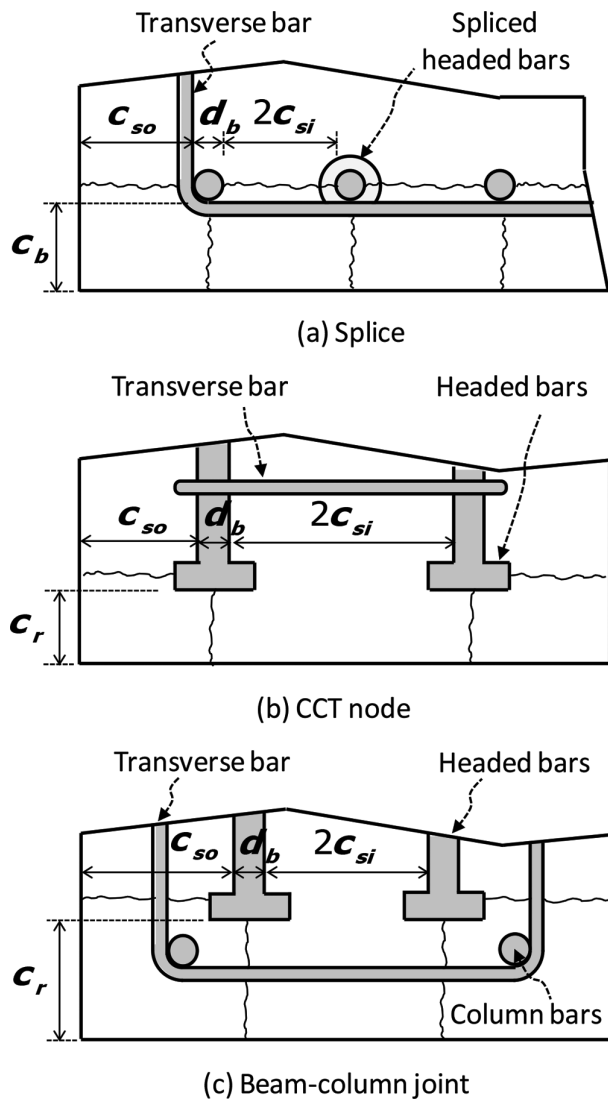


Fig. 2—Effect of cover concrete on bond strength.

where $l_{m0} = \max(0.3d_b f_y / (4f_{bd}), 10d_b, 100 \text{ mm})$; η_3 is coefficient of diameter of the bar ($= (25/d_b)^{0.3} \leq 1.0$); η_4 is coefficient of yield strength of the bar ($= 0.68$ to 1.2); $c_d = \min(c_{so}, c_{si})$; c_{so} is thickness of the side cover concrete; c_{si} is one-half of the clear bar spacing; $c_m = \max(c_{so}, c_{si})$; k_d is coefficient of the arrangement of the transverse reinforcement ($= 0$ to 20); α_t is coefficient of the transverse bar diameter ($= 0.5$ for D25 [diameter = 25 mm] to 1.0 for D50); A_{tr} is total cross-sectional area of transverse bars within spacing s_t ; s_t is center-to-center distance between the transverse bars; and n is the number of headed bars. A partial safety factor for the concrete ($f_{bd0}/1.5$) is considered in Eq. (2c).

In the study by Thompson et al.,¹⁰ overall anchorage strength of a headed bar is defined as the sum of the head bearing force and the bond strength of the straight bar length, and the development length l_d of a headed bar is calculated from the development length l_s of an equivalent straight bar

$$l_d = \frac{l_s}{\chi_y} (f_y - f_{head}) \quad (3a)$$

$$\chi = 1 - 0.7 \left(\frac{A_{nh}}{5A_b} \right) \geq 0.3 \quad (3b)$$

$$f_{head} = 2n_{5\%} f_c \psi \left(\frac{c}{d_b} \right) \sqrt{\frac{A_{nh}}{A_b}} \quad (3c)$$

$$\psi = 0.6 + 0.4(c_2/c) \leq 2.0 \quad (3d)$$

where l_s is development length of an equivalent straight bar; A_{nh} is net cross-sectional area of the head; A_b is cross-sectional area of the reinforcing bar; $n_{5\%}$ is 5% fractile coefficient ($= 0.7$); c is minimum cover dimension measured from the bar center; and c_2 is minimum cover dimension in the direction orthogonal to c .

In the study by Shao et al.,¹⁵ the development length of a headed bar is defined as follows

$$l_d = 0.0199 \frac{f_y \Psi_e \Psi_{cs} \Psi_o}{\sqrt[4]{f'_c}} d_b^{1.5} \quad (\text{in MPa and mm}) \quad (4a)$$

$$\Psi_{cs} = \frac{1}{12} \left(14 - \frac{s}{d_b} \right) \quad \text{without lateral confinement} \quad (4b)$$

$$\Psi_{cs} = \frac{1}{20} \left(18 - \frac{s}{d_b} \right) \left(1 - \frac{29.3}{f_y} \frac{A_{tr}}{A_{hs}} d_b^{0.75} \right) \quad (4c)$$

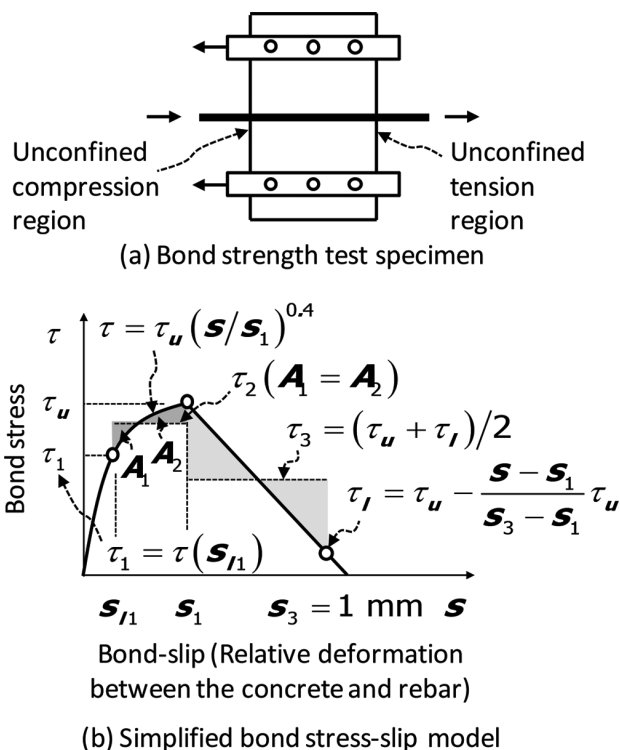
with lateral confinement (in MPa and mm)

where Ψ_o is coefficient of concrete cover ($= 1.0$ to 1.25); s is center-to-center spacing of headed bars ($= 2c_{si} + d_b \leq 8d_b$); A_{tr} is total cross-sectional area of all confining reinforcement parallel to l_d and located within $8d_b$ of the top or bottom of headed bars in the joint, or within $10d_b$ if d_b is greater than 28.7 mm (1.1 in) ($\leq 0.3A_{hs}$); A_{hs} is total cross-sectional area of headed bars; and $f_y = 414 \text{ MPa}$ (60 ksi) is used for low-strength reinforcing bars with $f_y < 414 \text{ MPa}$ (60 ksi).

PROPOSED METHOD FOR BAR DEVELOPMENT LENGTH

Spring model for head bearing

Head bearing and bond stress distribution in a headed bar anchorage are shown in Fig. 3(a). Under a tension force, the head bearing restrains bond-slip between the reinforcing bar and concrete. However, the bearing force can cause pullout failure or side-face blowout failure of the cover concrete. As the relative displacement between the headed bar and concrete (that is, bar-slip) increases, the bearing stress of the head and the bond stress of the straight bar increase. Ultimately, the headed bar strength is determined as the sum of the peak bearing strength and the bond strength reduced by large bar-slip.^{7,9} Thus, the anchorage effect of the head needs to be considered when evaluating development length of headed bars. Figure 3(b) shows the proposed straight bar model with a spring (that is, head bearing) used to describe pullout resistance of a headed bar. The tension force of a headed bar is resisted by the damaged and undamaged bond


$$\tau_u = 0.91\alpha_d \sqrt{f'_c} \quad (\text{in MPa}) \quad (5)$$

$$s_1 = 0.3\sqrt{f'_c/30} \text{ (in MPa and mm)} \quad (6)$$

where $\alpha_d = 1.1$ for D19 bars (that is, $d_b = 19$ mm) or less, 1.0 for D22 to D29 bars, and 0.9 for D32 bars or greater. The bond stress no longer exists at $s_3 = 1$ mm.¹⁸ For new concrete materials or reinforcing bars, the unit bond stress-slip relationship of a reinforcing bar should be redefined by pullout tests of materials.^{16,17} In fact, the bond-slip s_1 and s_3 are affected by other parameters, including reinforcing bar diameter and rib area. Thus, further studies are required.

Figure 5(b) shows the nonuniform bond stress distribution of a headed bar with a development length l_d in Fig. 5(a). The relative displacement between the headed bar and concrete is increased along the length from the unloaded end to the loaded end of the headed bar. In the unloaded region (that is, head) of the headed bar, the bond stress is increased with increasing the relative displacement (refer to the ascending branch in Fig. 4(b)). On the other hand, the relative displacement at the loaded end of the headed bar exceeds the displacement corresponding to the peak bond strength. Thus, the bond stress is decreased due to the local bond damage (see the descending branch in Fig. 4(b)). To describe the variation of the bond stresses in the development length l_d of the headed bar, the bond stress distribution was simplified with three uniform stresses: undamaged bond stress τ_1 at the bearing region length l_1 , undamaged bond stress τ_2 at l_2 , and damaged bond stress τ_3 at l_3 (refer to Fig. 5(c)). For

Figure 4 shows a simplified monotonic envelop curve proposed by Eligehausen et al.,¹⁹ on the basis of existing bar-slip test results under monotonic push-pull loading or cyclic loading.²⁰ Using the simplified bond stress-slip relationship, Hwang et al.^{16,17} proposed a nonuniform bond stress distribution model for the development length of straight and hooked reinforcing bars. In Fig. 4(b), the peak bond stress τ_u and bond-slip s_1 are defined as follows

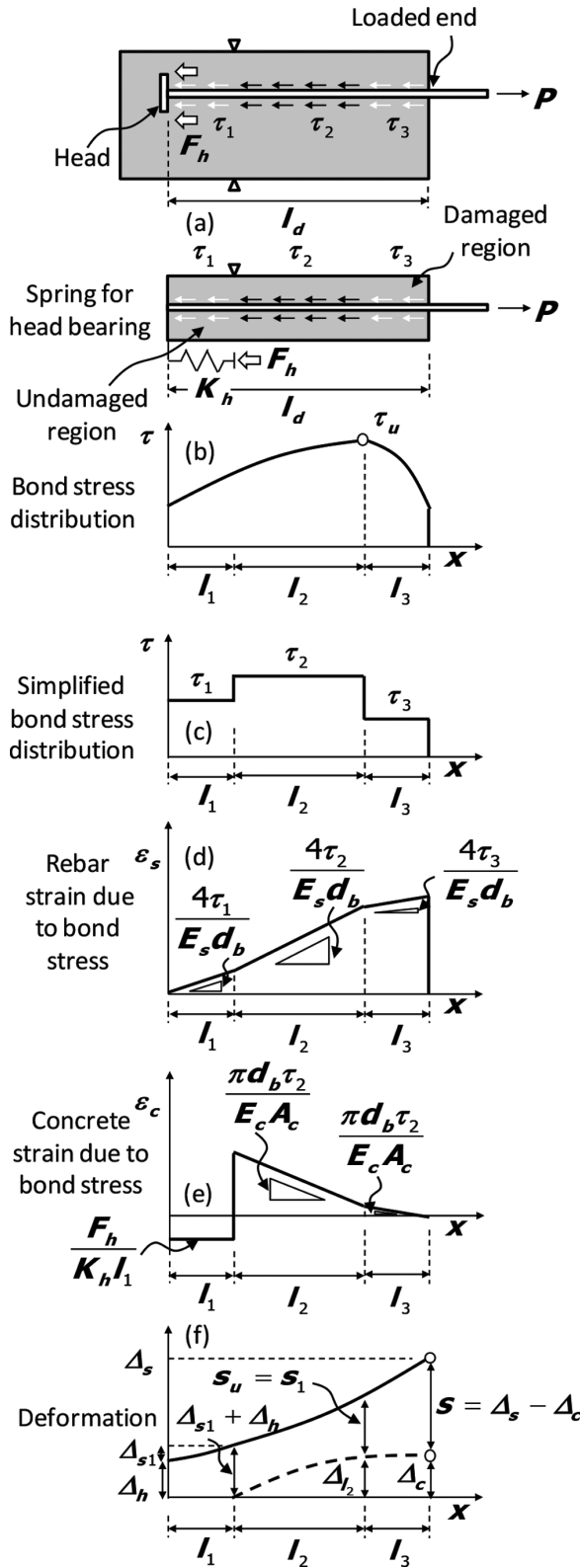


Fig. 5—Proposed bond stress distribution model.

simple calculation, these three bond stresses were assumed to be uniformly distributed. Hwang et al.¹⁶ reported that the rigorous non-linear bond stress model in Fig. 5(b) and the average bond stress model in Fig. 5(c) resulted in the same

development length. Thus, in the present study, the average bond stress distribution model was used to develop a simplified design equation.

For a reinforcing bar, the relationship between the bar stress and bond stress is defined as follows

$$\left(\frac{\pi d_b^2}{4} \right) \frac{d\sigma_s}{dx} = \tau(x)(\pi d_b) \quad (7)$$

where σ_s is tensile stress of the reinforcing bar. Considering the bearing force F_h of the head and the simplified bond stress distribution shown in Fig. 5(c), and assuming elastic behavior of materials, the strain distributions of the reinforcing bar and concrete are determined as shown in Fig. 5(d) and (e).

The relative displacement s between the reinforcing bar and concrete due to bar-slip is defined from the difference of strains.

$$\varepsilon_s - \varepsilon_c = ds/dx \quad (8)$$

The absolute displacement Δ_s of the reinforcing bar at the loaded end (that is, at $x = l_d$) is calculated from the strain distribution of the reinforcing bar in Fig. 5(d)

$$\begin{aligned} \Delta_s &= \int_0^{l_1} \frac{4\tau_1}{E_s d_b} x dx + \int_{l_1}^{l_1+l_2} \frac{4[\tau_1 l_1 + \tau_2(x-l_1)]}{E_s d_b} dx \\ &\quad + \int_{l_1+l_2}^{l_1+l_2+l_3} \frac{4[\tau_1 l_1 + \tau_2 l_2 + \tau_3(x-l_2)]}{E_s d_b} dx + \Delta_h \\ &= \frac{2}{E_s d_b} [(l_1 + 2l_2 + 2l_3)l_1 \tau_1 + (l_2 + 2l_3)l_2 \tau_2 + l_3^2 \tau_3] + \Delta_h \end{aligned} \quad (9)$$

where Δ_h is absolute displacement of the reinforcing bar at the head of the headed bar (that is, at $x = 0$); and Δ_s is defined as the sum of the deformations of the reinforcing bars in the three bond regions and the deformation of the spring due to the bearing force of the head.

At the loaded end ($x = l$), the relative displacement s between the reinforcing bar and concrete is defined from Eq. (8) (refer to Fig. 5(f)).

$$s = \Delta_s - \Delta_c \quad (10)$$

The peak bond stress τ_u is assumed to occur at $x = l_1 + l_2$ (refer to Fig. 5(b)), in which the relative displacement s_u reaches s_1 (refer to Fig. 4(b)). Thus, s_u at $x = l_1 + l_2$ can be estimated as follows (refer to Fig. 5(f))

$$\begin{aligned} s_u &= \int_0^{l_1} \frac{4\tau_1}{E_s d_b} x dx + \int_{l_1}^{l_1+l_2} \frac{4[\tau_1 l_1 + \tau_2(x-l_1)]}{E_s d_b} dx + \Delta_h - \Delta_{l_2} \\ &= \frac{2}{E_s d_b} (l_1^2 \tau_1 + 2l_1 l_2 \tau_1 + l_2^2 \tau_2) + \Delta_h - \Delta_{l_2} \approx s_1 \end{aligned} \quad (11)$$

where Δ_{l_2} is absolute tensile displacement of the concrete at $x = l_1 + l_2$. According to previous studies by Hwang et al.,^{16,17} Δ_{l_2} can be regarded as the overall displacement of concrete

Δ_c at $x = l_d$, considering a small distance between $x = l_1 + l_2$ and l_d : $\Delta_{l_2} = \Delta_c$.

After inserting Eq. (11) and $\Delta_{l_2} = \Delta_c$ into Eq. (9) and (10), the relative displacement s at the loaded end is defined as follows

$$s = \frac{2}{E_s d_b} [2l_1 l_3 \tau_1 + 2l_2 l_3 \tau_2 + l_3^2 \tau_3] + s_1 \quad (12)$$

As shown in Fig. 4(b), the bond stress τ_3 decreases with the increase of the relative displacement in the damaged region ($x = l_1 + l_2$ to l_d). For simplicity, the damaged bond stress τ_3 is defined as the average bond stress between the peak bond stress τ_u and the bond stress τ_l corresponding to the relative displacement s at the loaded end ($x = l_d$)^{16,17}

$$\tau_l = \tau_u - \frac{s - s_1}{s_3 - s_1} \tau_u = \frac{1 - C_1 [4l_1 \tau_1 + 4l_2 \tau_2 + l_3 \tau_u]}{1/\tau_u + C_1 l_3} \geq 0 \quad (13a)$$

$$\tau_3 = \frac{\tau_u + \tau_l}{2} = \frac{1 - 2C_1 [l_1 \tau_1 + l_2 \tau_2]}{1/\tau_u + C_1 l_3} \geq \frac{\tau_u}{2} \quad (13b)$$

where $C_1 = l_3 / [(1 - s_1)E_s d_b]$.

Similarly, in the effective bearing length from $x = 0$ to l_1 , the bond stress τ_1 is defined as the average bond stress between the bond stress corresponding to the absolute displacement Δ_h of the head at $x = 0$ and the bond stress corresponding to the relative displacement $s_{l1} = \Delta_{s1} + \Delta_h$ at $x = l_1$.

$$\begin{aligned} \tau_1 &= \frac{1}{s_{l1} - \Delta_h} \int_{\Delta_h}^{s_{l1}} \tau_u \left(\frac{s}{s_1} \right)^{0.4} ds \\ &= \frac{\tau_u}{1.4} \left(\frac{s_{l1}}{s_1} \right)^{0.4} \left[\frac{1 - (\Delta_h/s_{l1})^{1.4}}{1 - (\Delta_h/s_{l1})} \right] \quad (\text{in MPa and mm}) \end{aligned} \quad (14a)$$

In the undamaged region from $x = l_1$ to $l_1 + l_2$, as shown in Fig. 4(b), the bond stress τ_2 is defined as the average bond stress between the bond stress corresponding to the relative displacement $s_{l1} = \Delta_{s1} + \Delta_h$ at $x = l_1$ and the peak bond stress τ_u at $x = l_1 + l_2$.

$$\begin{aligned} \tau_2 &= \frac{1}{s_1 - s_{l1}} \int_{s_{l1}}^{s_1} \tau_u \left(\frac{s}{s_1} \right)^{0.4} ds \\ &= \frac{\tau_u}{1.4} \left[\frac{1 - (s_{l1}/s_1)^{1.4}}{1 - (s_{l1}/s_1)} \right] \quad (\text{in MPa and mm}) \end{aligned} \quad (14b)$$

The relative displacement $s_{l1} = \Delta_{s1} + \Delta_h$ can be calculated by assuming a uniform value of Δ_h along l_1 in Fig. 5(f)

$$s_{l1} = \Delta_{s1} + \Delta_h = \frac{2\tau_1 l_1^2}{E_s d_b} + \frac{F_h}{K_h} \quad (15a)$$

where F_h is the bearing force of the head; and K_h is the bearing stiffness of the concrete in the effective bearing length (refer to the section “Effect of head anchorage”).

Equations (14a) and (15a) are coupled. Thus, to calculate the average undamaged bond stress τ_1 from Δ_h and s_{l1} , iterative calculations are necessary. In the present study, for simplicity and safe estimation, the absolute displacement Δ_{s1} of reinforcing bar is neglected, assuming the lowest value $\tau_1 = 0$ in Eq. (15a). Thus, s_{l1} in Eq. (15a) can be explicitly defined as follows.

$$\frac{s_{l1}}{s_1} \approx \frac{F_h}{s_1 K_h} \leq 1 \quad (\text{in MPa and mm}) \quad (15b)$$

Using $s_{l1} \approx \Delta_h$ from Eq. (15b), τ_1 in Eq. (14a) can be simplified as follows.

$$\tau_1 = \tau_u \left(\frac{s_{l1}}{s_1} \right)^{0.4} \quad (15c)$$

In a headed bar, the maximum tensile strength f_s of the reinforcing bar can be defined as a function of τ_1 , τ_2 , τ_3 , l_1 , l_2 , l_3 , and F_h (refer to Fig. 5(c)).

$$f_s = \frac{4}{d_b} [\tau_1 l_1 + \tau_2 l_2 + \tau_3 l_3] + F_h \quad (16)$$

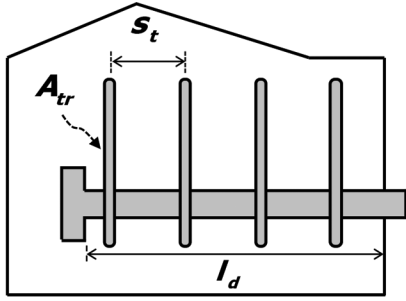
In Eq. (16), the ratio of the undamaged length $l_1 + l_2$ to the development length l_d is required to calculate the maximum stress f_s . In the present study, $l_1 + l_2$ was simplified as $0.75l_d$ on the basis of a parametric study and the results of previous studies^{16,17} for the nonuniform bond stress distribution of straight bars (refer to Appendix A*).

Effect of cover concrete and transverse bars

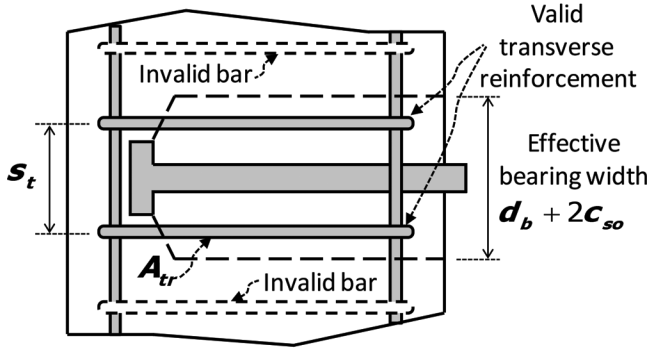
In reinforced concrete members without sufficient concrete cover or confinement of transverse reinforcement, the reinforcing bar bond strength is decreased due to splitting or blowout failure. Two or three strength modification coefficients are used in current design codes to address the effects of concrete cover and transverse reinforcement. In the present study, for better predictions, the coefficients proposed by Hwang et al.^{16,17} were applied to the proposed model to address such effects. According to the anchorage location of the headed bar, coefficients of headed bars were classified into the following: 1) lap splice; and 2) CCT node and beam-column joint.

Figure 6 shows the effect of transverse reinforcement. In the case of confining bars perpendicular to the headed bar, all the transverse bars are considered in the calculation of development length of the headed bar (refer to Fig. 6(a)). On the other hand, when confining bars are parallel to the headed bar, only the confining bars within the effective bearing width are assumed to be valid (refer to Fig. 6(b)).

*The Appendix is available at www.concrete.org/publications in PDF format, appended to the online version of the published paper. It is also available in hard copy from ACI headquarters for a fee equal to the cost of reproduction plus handling at the time of the request.



(a) Confining bars perpendicular to the headed bar



(b) Confining bars parallel to the headed bar

Fig. 6—Effect of confining bars on bond strength.

When headed bars are used for lap splice, the reduction coefficient proposed in ACI 408R-03²¹ is used to redefine the peak bond stress τ_u decreased by splitting or blowout failure¹⁶

$$\tau_u = 0.91\alpha_d \sqrt{f'_c} \left[\frac{(c_0 w + K_{atr})/d_b}{2.5} \right] \quad (\text{in MPa and mm}) \quad (17a)$$

$$(c_0 w + K_{atr})/d_b \leq 4.0 \quad (17b)$$

$$w = 0.1(c_{max}/c_{min}) + 0.9 \leq 1.25 \quad (17c)$$

$$K_{atr} = (0.18d_b + 1.32)\sqrt{f'_c}A_{tr}/(s_t n) \quad (\text{in MPa and mm}) \quad (17d)$$

where $c_0 = c_{min} + d_b/2$; $c_{max} = \max(c_b, c_s)$; $c_{min} = \min(c_b, c_s)$; and $c_s = \min(c_{so}, c_{si} + 6.4)$.

When headed bars are used in CCT node and beam-column joint, the reduction coefficient proposed by Hwang et al.¹⁷ is used to redefine the peak bond stress τ_u decreased by blowout failure

$$\tau_u = \frac{0.91\alpha_d \sqrt{f'_c}}{\alpha_{m1}\alpha_{m2}\alpha_{m3}} \quad (\text{in MPa and mm}) \quad (18a)$$

$$\alpha_{m2} = 0.7 \leq 1 - 0.1(c_d/d_b - 1) \leq 1.0 \quad (18b)$$

$$\alpha_{m3} = 0.7 \leq 1 - 0.3(\sum A_{tr} - 0.25A_s)/A_s \leq 1.0 \quad (18c)$$

where α_{m1} is coefficient of the rear concrete cover ($= 0.85$ for $c_r > d_b$, otherwise 1.0); and $\alpha_{m2}\alpha_{m3} \geq 0.7$.

Effect of head anchorage

When a headed bar is subjected to a pullout force, the bearing force of the head is determined by the bearing strength, side blowout resistance, or concrete breakout resistance.

$$F_h = \min(F_{b1}, F_{b2}) \quad (19a)$$

Thompson et al.⁸ proposed the concrete bearing strength F_{b1} of a head based on more than 500 existing pull-out test results of unbonded anchor bolts or headed bars and compression tests of bearing plate on concrete blocks (Eq. (3c)).

$$F_{b1} = 4n_{5\%}f'_c \left(0.3 + \frac{c_2}{5c} \right) \left(\frac{c}{d_b} \right) \sqrt{\frac{A_{nh}}{A_b}} \leq 4n_{5\%}f'_c \left(\frac{c}{d_b} \right) \sqrt{\frac{A_{nh}}{A_b}} \quad (19b)$$

where fractile coefficient $n_{5\%} = 1.0$ is used; $c = \min(c_b, c_{so}, c_{si})/d_b + 0.5$; and c_2 is minimum cover dimension in the direction orthogonal to c ($= c_b/d_b + 0.5$ or $c_{so}/d_b + 0.5$) in CCT node and lap splice. In beam-column joint, $c = \min(c_{so}, c_{si})/d_b + 0.5$; and $c_2 = c_{so}/d_b + 0.5$, which is related to side blowout failure.

ACI 318-14¹ defines the concrete breakout strength F_{b2} of anchors, headed studs, and headed bolts on the basis of the fracture mechanism and existing shallow embedment pullout test results of unbonded headed reinforcement.

$$\begin{aligned} F_{b2} &= \psi \frac{A_{Nc}}{9l_d^2} \frac{1.25}{nA_b} \left(0.7 + 0.3 \frac{c}{1.5l_d} \right) (10\sqrt{f'_c}l_d^{1.5}) \\ &= \psi \frac{A_{Nc}\sqrt{f'_c}}{0.72nA_b\sqrt{l_d}} \left(0.7 + \frac{c}{5l_d} \right) \end{aligned} \quad (\text{in MPa and mm}) \quad (19c)$$

In this equation, this study proposes the factor ψ to address the effects of reinforcement and loading conditions in the concrete failure area (not the same as the condition of the anchorage in plain concrete). The concrete breakout strength can be increased by the compressive strut in CCT node, compression force of the opposite head bearing in lap splice, column reinforcing bars and compression zone of beam in beam-column joint, or relatively large tensile strength of steel fiber-reinforced concrete. Based on existing test results, $\psi = 2.5$ for beam-column joint using ordinary concrete and $\psi = 5$ for CCT node, lap splice, or beam-column joint using steel fiber-reinforced UHPC were used in this study. A_{Nc} is projected concrete failure area. In CCT node and lap splice, A_{Nc} is defined as $b_b \times \min(c_b + 0.5d_b + 1.5l_d, h_b)$, where b_b is beam width and h_b is beam depth.¹ In beam-column joint, A_{Nc} is defined as $3b_cl_d$, where b_c is column width.¹

Concrete bearing strength F_{b1} (Eq. (19b)) and concrete breakout strength F_{b2} (Eq. (19c)) were applied to existing test specimens. The results showed that failure was determined by F_{b2} for most of the test specimens (344 out of 361 specimens). Thus, in the proposed model, the bearing strength of the head was simplified as $F_h = F_{b2}$.

In Eq. (15), the bearing stiffness can be simplified as the axial stiffness of the concrete with a net head area A_{nh} in the effective bearing length l_1 (refer to Fig. 3(a))

$$K_h = \frac{E_c}{l_1} \left(\frac{A_{nh}}{A_b} \right) \approx \frac{E_c}{d_h} \left(\frac{A_{nh}}{A_b} \right) \quad (20)$$

where E_c is elastic modulus of concrete; and d_h is equivalent diameter of the circular head ($= \sqrt{[4(A_{nh} + 1)/\pi]}$).

Summary of proposed method

The proposed method is summarized as follows using $l_1 + l_2 = 0.75l_d$ and $l_3 = 0.25l_d$ in Eq. (13b) and Eq. (14) to (20)

$$f_s = \frac{l_d}{d_b} \left[(\tau_1 - \tau_2) \frac{4d_h}{l_d} + 3\tau_2 + \tau_3 \right] + F_h \leq f_y \quad (21a)$$

$$\tau_1 = \tau_u \left(\frac{s_{l1}}{s_1} \right)^{0.4} \quad (\text{in MPa and mm}) \quad (21b)$$

$$\tau_2 = \frac{\tau_u}{1.4} \left[\frac{1 - (s_{l1}/s_1)^{1.4}}{1 - (s_{l1}/s_1)} \right] \leq \tau_u \quad (\text{in MPa and mm}) \quad (21c)$$

$$\tau_3 = \left\{ \frac{4 - C_1[8d_h(\tau_1 - \tau_2) + 6l_d\tau_2]}{4 + C_1l_d\tau_u} \right\} \tau_u \geq \frac{\tau_u}{2} \quad (21d)$$

$$\tau_u = 0.91\alpha_d \sqrt{f'_c} \left[\frac{(c_0 w + K_{atr})/d_b}{2.5} \right] \text{ for lap splice (in MPa)} \quad (21e)$$

$$\tau_u = \frac{0.91\alpha_d \sqrt{f'_c}}{\alpha_{m1}\alpha_{m2}\alpha_{m3}} \text{ for CCT node and beam-column joint (in MPa)} \quad (21f)$$

$$\frac{s_{l1}}{s_1} \approx \frac{F_h}{s_1} \frac{d_h}{E_c} \left(\frac{1}{A_{nh}/A_b} \right) = \frac{F_h d_h}{257 f'_c} \left(\frac{1}{A_{nh}/A_b} \right) \leq 1 \quad (\text{in MPa and mm}) \quad (21g)$$

$$F_h = \psi \frac{A_{Nc} \sqrt{f'_c}}{0.72 n A_b \sqrt{l_d}} \left(0.7 + \frac{c}{5l_d} \right) \quad (\text{in MPa and mm}) \quad (21h)$$

where $C_1 = l_d[4(1 - \sqrt{0.003f'_c})E_s d_b]$. It is noted that when smaller or larger net head bearing area is used, tests should be performed to estimate the head anchorage force F_h . Then, the development length of the headed bars can be calculated using the test strength of head anchorage. The larger net head area A_{nh} decreases s_{l1}/s_1 at the peak stress. Under

reversed cyclic loading, the bond demand can be increased by the effects of bond degradation and cyclic strain hardening of the reinforcing bars. Thus, further studies of the post-yield bond behavior are required.

In the proposed method (Eq. (21a)), the calculation of the bar stress from an assumed development length is more convenient than the development length calculation from the bar stress. Thus, in the process of finding the development length corresponding to a given bar yield strength, iterative calculations are necessary. Values of the design parameters are presented in Table B1 of Appendix B, from which the bar stress can be conveniently calculated without using Eq. (21). For given design parameters, three bond stresses and bearing stress of the head are calculated in sequence from the top to bottom. When each parameter is between two values, interpolation can be used (for example, from $(c_0 w + K_{atr})/d_b = 1.5$, $\tau_u/(\alpha_d \sqrt{f'_c}) = (0.364 + 0.725)/2$). If new concrete materials or reinforcing bars are used, the unit bond strength τ_u should be defined by performing pullout tests, differently from Eq. (21e) and (21f) for ordinary concrete materials or reinforcing bars.^{16,17}

For ordinary concrete without fiber reinforcement (concrete strength $f'_c = 20.3$ to 226.0 MPa [2.9 to 32.8 ksi]), Eq. (21) can be further simplified using empirical values of design parameters obtained from the comparison between the proposed method and existing test results. Considering the parameters of existing test specimens, the average value of s_{l1}/s_1 in Eq. (21g) was estimated to be 0.344 , which resulted in $\tau_1 = 0.653\tau_u$ and $\tau_2 = 0.844\tau_u$ in Eq. (21b) and (21c), respectively. Because the contribution of the damaged bond stress τ_3 was relatively small, the minimum value $\tau_3 = 0.5\tau_u$ was used for τ_3 in Eq. (21d). $A_{Nc} = b_b h_b$ was used for CCT node and lap splice while $A_{Nc} = 3b_c l_d$ was used for beam-column joint in Eq. (21h).

Using these parameters, Eq. (21) can be simplified as follows

$$f_s = 3\tau_u \frac{l_d}{d_b} + F_h \leq f_y \quad (22a)$$

$$\tau_u = 0.91\alpha_d \sqrt{f'_c} \left[\frac{(c_0 w + K_{atr})/d_b}{2.5} \right] \text{ for lap splice (in MPa)} \quad (22b)$$

$$\tau_u = \frac{0.91\alpha_d \sqrt{f'_c}}{\alpha_{m1}\alpha_{m2}\alpha_{m3}} \text{ for CCT node and beam-column joint (in MPa)} \quad (22c)$$

$$F_h = \frac{8.8b_b h_b \sqrt{f'_c}}{n d_b^2 \sqrt{l_d}} \left[0.7 + \frac{\min(c_b, c_{so})}{5l_d} \right]$$

for CCT node and lap splice (in MPa and mm) (22d)

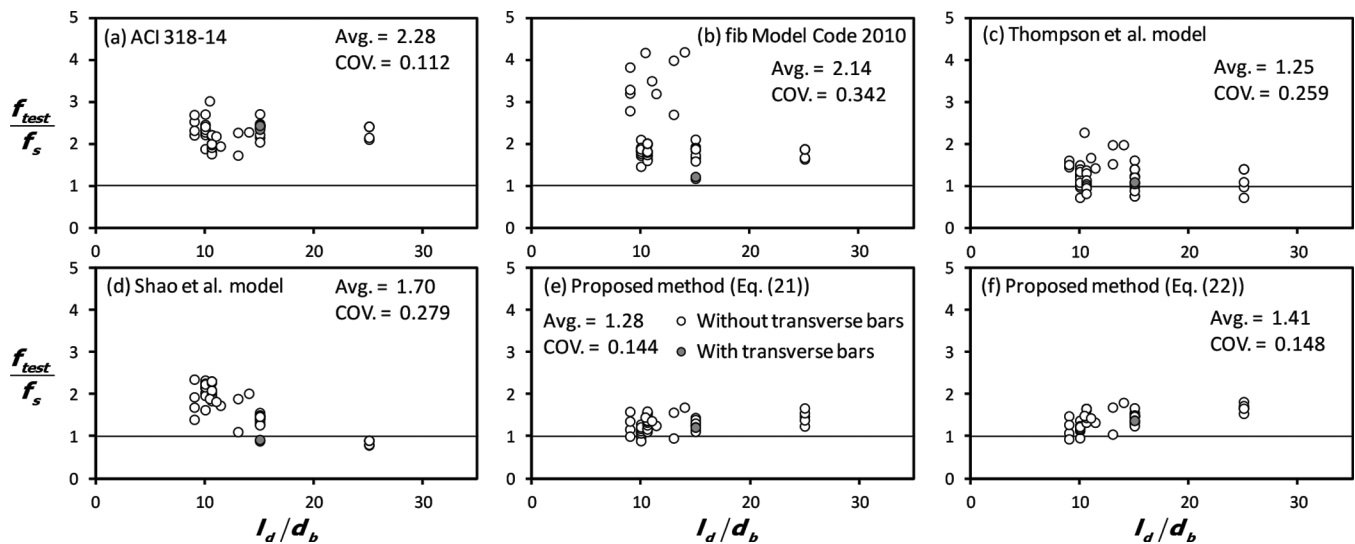


Fig. 7—Headed bar stress ratio of CCT node test specimens.

$$F_{sh} = \frac{13.3b_c \sqrt{l_d} \sqrt{f'_c}}{nd_b^2} \left(0.7 + \frac{c_{so}}{5l_d} \right)$$

for beam-column joint using ordinary concrete
(in MPa and mm) (22e)

$$F_{sh} = \frac{26.5b_c \sqrt{l_d} \sqrt{f'_c}}{nd_b^2} \left(0.7 + \frac{c_{so}}{5l_d} \right)$$

for beam-column joint using SFR-UHPC (in MPa and mm)
(22f)

where l_d is the development length measured from the critical section to the inside face of the head.

Using $f_s = f_y$ in Eq. (22), the development length l_d for the yield strength of a headed bar is directly estimated from the reinforcing bar stress without iterative calculations.

$$l_d = \left(\frac{f_y - F_{sh}}{3\tau_u} \right) d_b \geq 0 \quad (23)$$

COMPARISON BETWEEN TEST RESULTS AND PREDICTIONS

To verify the validity of the proposed method, it was applied to existing test specimens for headed bars (refer to Fig. 1). Test specimens showing joint shear failure or early spalling of plain concrete (without reinforcement in the specimens) were excluded because such failure modes do not represent pure bond mechanism of headed bars. In Appendix C, Table C1 presents the test parameters. Ranges of these parameters are as follows: the development length $l_d = 89$ to 917 mm (3.5 to 36.1 in.), headed bar diameter $d_b = 15.9$ to 57.3 mm (0.6 to 2.3 in.), net head area-to-reinforcing bar area $A_{nh}/A_b = 1.1$ to 14.9, concrete strength $f'_c = 20.3$ to 226.0 MPa (2.9 to 32.8 ksi), and yield strength of the reinforcing bar $f_y = 433$ to 959 MPa (62.8 to 139.1 ksi).^{3,5,8,9,12-15} For 50 CCT node specimens, 40 lap splice specimens, and 271 beam-column joint specimens, the tensile strengths f_s of the headed bars were calculated according to the given development

lengths. For several specimens, the tensile strengths f_s were measured at a location shorter than the development length. In such cases, the tensile strengths f_s were calculated at the measurement location.

Table C2 compares the predictions of existing design methods and the proposed method with the test results. In Model Code 2010² and Thompson et al.,¹⁰ safety factors were not considered for direct comparison with test results.

Figures 7, 8, and 9 compare the test results with the bar stress predictions of existing design methods and the proposed method. Figure 7 shows the ratios of the test strength to the prediction for CCT node specimens. In this figure, the specimens were classified as headed bars with or without transverse reinforcement. ACI 318-14,¹ Model Code 2010,² and Shao et al.¹⁵ model generally underestimated the strengths of the headed bars. Although safety factors were not included in the design equations, the prediction results were relatively conservative regardless of the development length-to-diameter ratio l_d/d_b . The proposed models in Eq. (21) and Eq. (22) predicted the test results with reasonable precision, showing an average ratio of 1.28 and 1.41, respectively, with COV. of 0.144 and 0.148, respectively.

Figure 8 shows the strength ratios for lap splice specimens. Unlike CCT node specimens, ACI 318-14¹ significantly overestimated the strengths of the headed bars at large development length-to-diameter ratio l_d/d_b . On the other hand, *fib* Model Code 2010² underestimated the strengths of the headed bars at large development length-to-diameter ratios l_d/d_b . The predictions of Shao et al.¹⁵ and the proposed methods in Eq. (21) and Eq. (22) were better than those with other design methods, showing an average ratio of 1.07, 1.03, and 1.07, respectively, with COVs of 0.204, 0.159, and 0.150, respectively.

Figure 9 shows the strength ratios for beam-column joint specimens. Test results marked in square and triangle indicate headed bars with large diameter of $d_b = 43$ and 57.3 mm (1.7 and 2.3 in.) and with steel fiber-reinforced UHPC of $f'_c = 130$ and 226 MPa (18.9 and 32.8 ksi), respectively. Generally, ACI 318-14¹ and Model Code 2010² underestimated the strengths of the headed bars. Particularly,

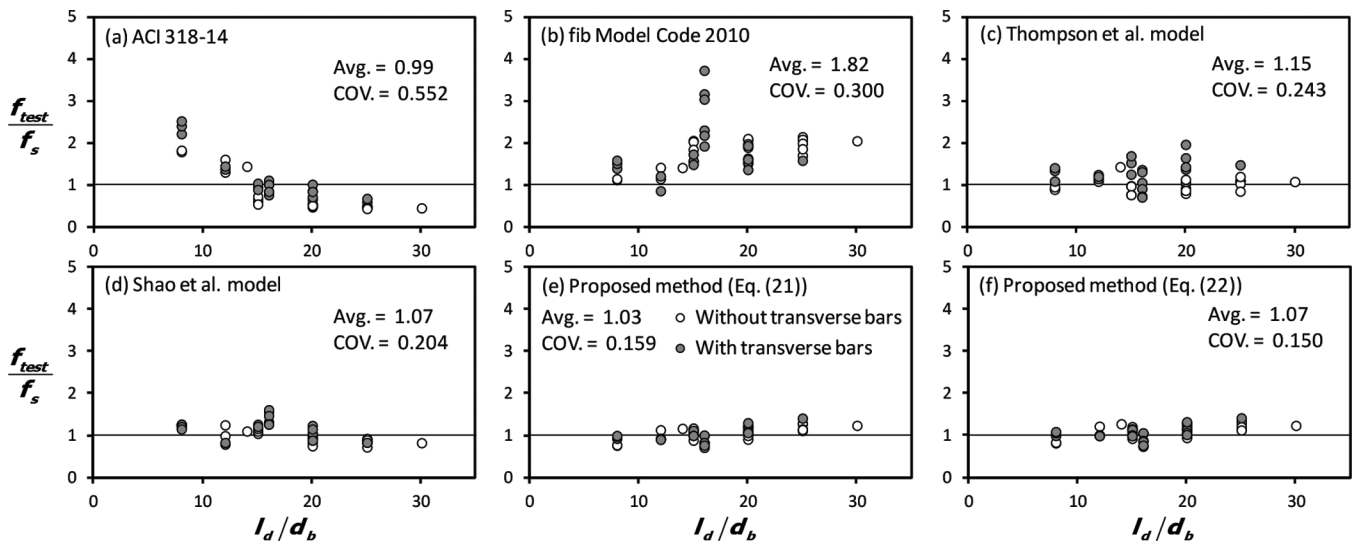


Fig. 8—Headed bar stress ratio of lap splice test specimens.

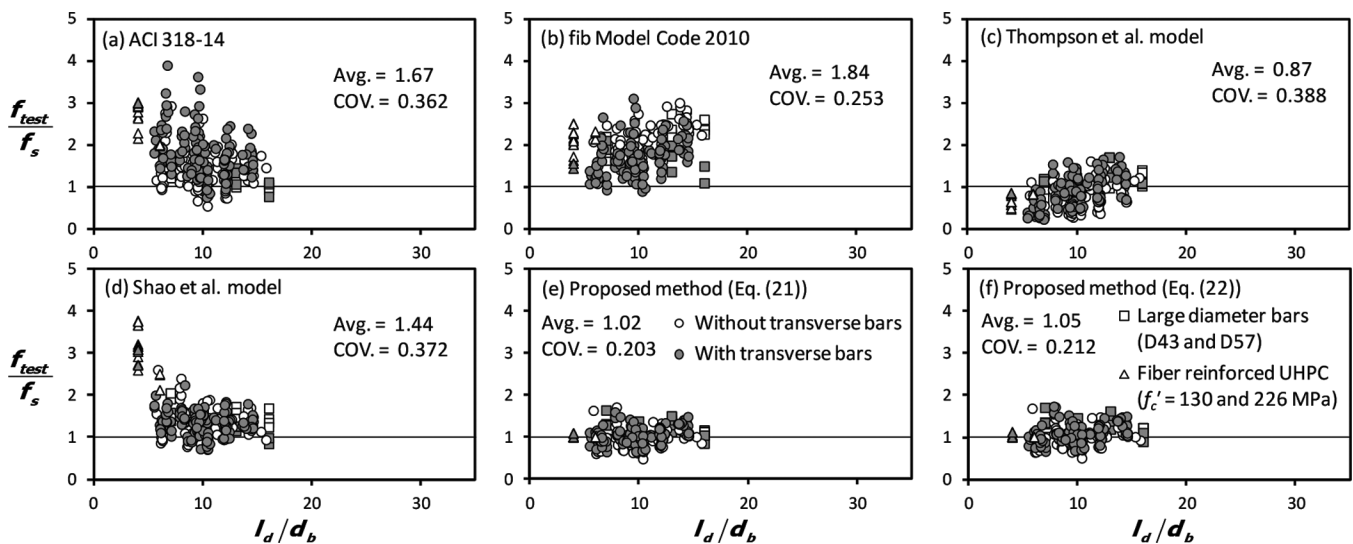


Fig. 9—Headed bar stress ratio of beam-column joint test specimens.

as development length-to-diameter ratio l_d/d_b decreased, ACI 318-14¹ significantly underestimated the strengths of the headed bars. Thompson et al.¹⁰ model overestimated the strengths of the headed bars for most of the test specimens. The Shao et al.¹⁵ model underestimated the strengths of the headed bars, particularly for steel fiber-reinforced UHPC. The proposed methods in Eq. (21) and (22) predicted the test results with best precision, regardless of the diameter of reinforcing bars or concrete type, showing an average ratio of 1.02 and 1.05 with COVs of 0.203 and 0.212, respectively. Despite such accurate predictions, the proposed method gave unsafe predictions for the test results. Thus, a safety factor is required to use the proposed method in actual design applications.

Figure 10 compares the predictions and test results for all specimens. ACI 318-14¹ and Model Code 2010² were developed based on the limited number of test results. For this reason, the ACI 318-14¹ and Model Code 2010² predictions showed relatively large average ratios of 1.68 and 1.88 with COVs of 0.386 and 0.282, respectively. Shao et al.¹⁵ model

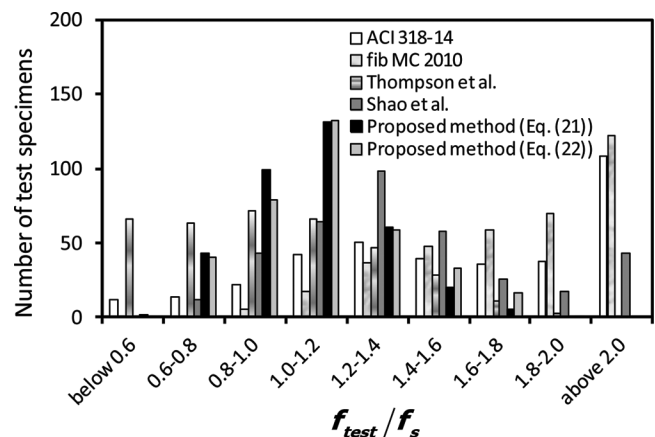


Fig. 10—Comparison of test results and predictions for existing headed bar test specimens.

showed an average ratio of 1.43 and a COV of 0.366 with stress ratio f_{test}/f_s of 0.8 to 1.8 for the majority of test specimens. The proposed model in Eq. (21) showed an average ratio of 1.06 and COV. of 0.207 with f_{test}/f_s of 0.6 to 1.4. The

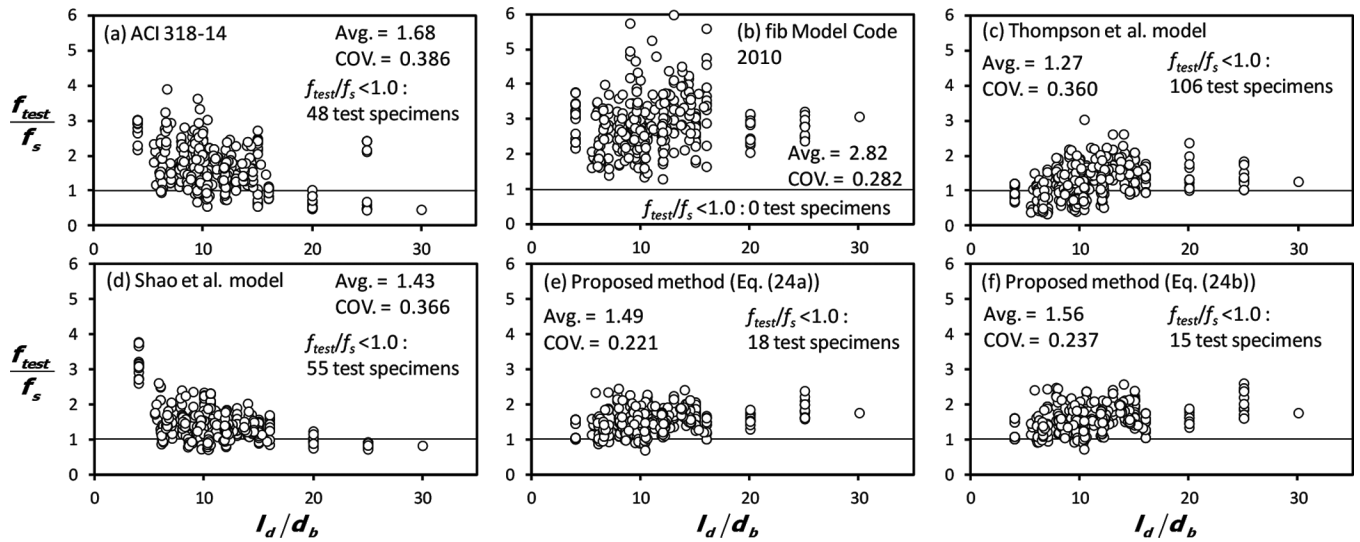


Fig. 11—Comparison of test results and predictions with safety factors for all test specimens.

proposed model in Eq. (22) showed an average ratio of 1.10 and COV of 0.225 with f_{test}/f_s of 0.6 to 1.4.

For safe design of actual structures, a safety factor $\phi = 0.7$ is recommended for Eq. (21) and (22) in the proposed method, on the basis of 5% fractile with 90% confidence level.

For the detailed method

$$f_s = \frac{\phi l_d}{d_b} \left[(\tau_1 - \tau_2) \frac{4d_h}{l_d} + 3\tau_2 + \tau_3 \right] + \phi F_h \leq f_y \quad (24a)$$

For the simplified method

$$f_s = \phi \left[3\tau_u \frac{l_d}{d_b} + F_{sh} \right] \leq f_y \quad (24b)$$

In Model Code 2010,² bond strengths are decreased to $f_{bd}/1.5$ in Eq. (2c) by using partial safety factor of concrete. In the Thompson et al. model,¹⁰ head bearing forces are decreased to 70% of nominal strengths by using 5% fractile coefficient of 0.7. In ACI 318-14¹ and the Shao et al.¹⁵ model, unlike other design methods, a safety factor is not used.

Figure 11 compares the prediction results with the safety factors. When $\phi = 0.7$ was used, the proposed models safely predicted the majority of the test results. The proposed methods in Eq. (24a) and Eq. (24b) overestimated the test strengths for 18 and 15 test specimens among the 361 test specimens, respectively. Their failure ratios were 5.0% and 4.2%, respectively. Using $\phi = 0.7$, the stress ratio of “average – $K \times$ standard deviation” for Eq. (24a) and Eq. (24b) was 0.950 and 0.954, respectively, which is close to 1.0 ($K = 1.645$ for 5% fractile [quantile] with 90% confidence level). Thus, the proposed methods satisfy the target safety level. On the other hand, the ACI 318 method overestimated test strengths of 48 specimens among 361 test specimens (Fig. 11): the failure ratio was 13.3%.

SUMMARY AND CONCLUSIONS

In the present study, a new design method was developed to predict the development lengths of headed bars. In the proposed method, a headed bar was idealized as a straight bar restrained by the spring model of the head. Following previous studies by the authors, a nonuniform bar bond stress distribution was considered. The bond stress distribution was simplified with three uniform bond stresses: two bond-undamaged regions of the effective bearing length and straight length and a bond-damaged region of the straight length. For the spring model of the head, the head strength was defined as the bearing strength of the head determined by blowout failure and breakout of the cover concrete. Using the bond stress distribution, unit bond strength, and bearing strength of the head, the tensile strength of the headed bar was defined as a function of the development length and head bearing force. To address the effects of cover concrete and transverse reinforcement on splitting or blowout failure, the relevant coefficients specified in ACI 408R and the authors’ previous study were used for the headed bars in lap splice, CCT node, and beam-column joint. To verify the validity of the proposed method, it was applied to 361 existing CCT node, lap splice, beam-column joint test specimens. In general, the prediction results of the proposed method agreed with the test results under various design conditions, including large diameter of reinforcing bars, fiber-reinforced high-strength concrete, and anchorage conditions (lap splice, CCT node, and beam-column joint) of headed bars. The accuracy of the proposed method (avg. = 1.06 and COV = 0.207) was better than that of existing design methods (avg. = 1.68 and COV = 0.386 in ACI 318). When a strength reduction factor of 0.7 was used, the failure ratio was not greater than 5.0%. In the proposed model, the effects of unit bond strength, bond stress distribution, and bearing resistance of the head were separately modeled. Such component models can be used in future experimental and theoretical studies.

AUTHOR BIOS

ACI member **Hyeon-Jong Hwang** is an Associate Professor in the College of Civil Engineering and Hunan Provincial Key Laboratory on Damage Diagnosis for Engineering Structures at Hunan University, Changsha, Hunan, China, and an Associate Researcher in the Engineering Research Institute at Seoul National University, Seoul, South Korea. He received his BE, MS, and PhD in architectural engineering from Seoul National University. His research interests include inelastic analysis and seismic design of reinforced concrete and composite structures.

Hong-Gun Park, FACI, is a Professor in the Department of Architecture & Architectural Engineering at Seoul National University. He received his BE and MS in architectural engineering from Seoul National University and PhD in civil engineering from the University of Texas at Austin, Austin, TX. His research interests include inelastic analysis and the seismic design of reinforced concrete structures.

Wei-Jian Yi is a Professor in the College of Civil Engineering at Hunan University. He received his BE, MS, and PhD at the College of Civil Engineering from Hunan University. His research interests include fundamental concrete structures and the seismic design of reinforced concrete structures.

ACKNOWLEDGMENTS

This research was financially supported by National Key Research Program of China (2016YFC0701400) and National Natural Science Foundation of China (Grant No. 51851110760 and 51338004). The authors are grateful to the authorities for their support.

NOTATION

A_b	=	cross-sectional area of headed bars, mm ² (in. ²)
A_{hs}	=	total cross-sectional area of headed bars, mm ² (in. ²)
A_{Nc}	=	projected concrete failure area, mm ² (in. ²)
A_{nh}	=	cross-sectional area of net head, mm ² (in. ²)
A_{tr}	=	cross-sectional area of transverse bars, mm ² (in. ²)
A_t	=	total cross-sectional area of transverse bars, mm ² (in. ²)
c	=	minimum cover dimension measured from bar center, mm (in.)
c_2	=	minimum cover dimension in direction orthogonal to c , mm (in.)
c_b	=	thickness of bottom cover concrete, mm (in.)
c_r	=	thickness of rear cover concrete, mm (in.)
c_{si}	=	one-half of center-to-center bar spacing, mm (in.)
c_{so}	=	thickness of side cover concrete, mm (in.)
d_b	=	reinforcing bar diameter, mm (in.)
d_h	=	equivalent diameter of circular shaped head, mm (in.)
E_c	=	elastic modulus of concrete, MPa (psi)
F_h	=	bearing strength of head, MPa (psi)
f'_c	=	concrete compressive strength, MPa (psi)
f_y	=	yield strength of reinforcing bar, MPa (psi)
K_h	=	stiffness of head, MPa/mm (psi/in)
k_d	=	coefficient of arrangement of transverse reinforcement
l_1	=	effective bearing length, mm (in.)
l_d	=	development length of headed bar, mm (in.)
l_s	=	calculated development length of straight bar, mm (in.)
n	=	number of headed bars
s	=	relative displacement between reinforcing bar and concrete, mm (in.)
s_1	=	bond-slip at peak bond stress, mm (in.)
s_t	=	center-to-center distance of transverse bars, mm (in.)
α_d	=	coefficient of reinforcing bar diameter in proposed model
α_{m1}	=	coefficient of rear concrete cover in proposed model
α_{m2}	=	coefficient of concrete cover in proposed model
α_{m3}	=	coefficient of transverse reinforcement in proposed model
α_t	=	coefficient of diameter of transverse reinforcement
Δ_h	=	absolute displacement of reinforcing bar due to head bearing, mm (in.)
Δ_s	=	absolute displacement of reinforcing bar at peak strength, mm (in.)
ϕ	=	safety factor
η_3	=	coefficient of reinforcing bar diameter in Model Code 2010
η_4	=	coefficient of yield strength of reinforcing bar
$\eta_{5\%}$	=	fractile coefficient
σ_s	=	tensile strength of reinforcing bar, MPa (psi)
τ_1	=	non-damaged bond stress at effective bearing length, MPa (psi)
τ_2	=	non-damaged bond stress at straight length, MPa (psi)

τ_3	=	damaged bond stress at straight length, MPa (psi)
τ_u	=	peak bond stress, MPa (psi)
Ψ	=	strength increment factor
Ψ_e	=	coefficient of epoxy-coated bars
Ψ_o	=	coefficient of concrete cover

REFERENCES

1. ACI Committee 318, "Building Code Requirements for Structural Concrete (ACI 318-14) and Commentary (ACI 318R-14)," American Concrete Institute, Farmington Hills, MI, 2014, 519 pp.
2. *fib*, "fib Model Code for Concrete Structures 2010," *fib*, Ernst & Sohn, Berlin, Germany, 2010, 420 pp.
3. Bashandy, T. R., "Application of Headed Bars in Concrete Members," PhD dissertation, University of Texas at Austin, Austin, TX, 1996, 302 pp.
4. Wright, J. L., and McCabe, S. L., "The Development Length and Anchorage Behavior of Headed Reinforcing Bars," *SM Report No. 44*, University of Kansas Center for Research, Lawrence, KS, Sept. 1997.
5. Choi, D. U.; Hong, S. G.; and Lee, C. Y., "Test of Headed Reinforcement in Pullout," *KCI Concrete Journal*, V. 14, No. 3, 2002, pp. 102-110.
6. Choi, D. U., "Test of Headed Reinforcement in Pullout II: Deep Embedment," *International Journal of Concrete Structures and Materials*, V. 18, No. 3, 2006, pp. 151-159.
7. Thompson, M. K.; Ziehl, M. J.; Jirsa, J. O.; and Breen, J. E., "CCT Nodes Anchored by Headed Bars-Part 1: Behavior of Nodes," *ACI Structural Journal*, V. 102, No. 6, Nov.-Dec. 2005, pp. 808-815.
8. Thompson, M. K.; Jirsa, J. O.; and Breen, J. E., "CCT Nodes Anchored by Headed Bars-Part 2: Capacity of Nodes," *ACI Structural Journal*, V. 103, No. 1, Jan.-Feb. 2006, pp. 65-73.
9. Thompson, M. K.; Ledesma, A.; Jirsa, J. O.; and Breen, J. E., "Lap Splices Anchored by Headed Bars," *ACI Structural Journal*, V. 103, No. 2, Mar.-Apr. 2006, pp. 271-279.
10. Thompson, M. K.; Jirsa, J. O.; and Breen, J. E., "Behavior and Capacity of Headed Reinforcement," *ACI Structural Journal*, V. 103, No. 4, July-Aug. 2006, pp. 522-530.
11. Hong, S. G.; Chun, S. C.; Lee, S. H.; and Oh, B., "Strut-and-Tie Model for Development of Headed Bars in Exterior Beam-Column Joint," *ACI Structural Journal*, V. 104, No. 5, Sept.-Oct. 2007, pp. 590-600.
12. Chun, S. C., "Lap Splice Tests Using High-Strength Headed Bars of 550 MPa (80 ksi) Yield Strength," *ACI Structural Journal*, V. 112, No. 6, Nov.-Dec. 2015, pp. 679-688. doi: 10.14359/51687936
13. Chun, S. C.; Choi, C. S.; and Jung, H. S., "Side-Face Blowout Failure of Large-Diameter High-Strength Headed Bars in Beam-Column Joints," *ACI Structural Journal*, V. 114, No. 1, Jan.-Feb. 2017, pp. 161-171. doi: 10.14359/51689161
14. Sim, H. J.; Chun, S. C.; and Choi, S., "Anchorage Strength of Headed Bars in Steel Fiber-Reinforced UHPC of 120 and 180 MPa," *Journal of the Korea Concrete Institute*, V. 28, No. 3, 2016, pp. 365-373. (in Korean). doi: 10.4334/JKCI.2016.28.3.365
15. Shao, Y.; Darwin, D.; O'Reilly, M.; Lequesne, R.; Ghimire, K.; and Hano, M., "Anchorage of Conventional and High-Strength Headed Reinforcing Bars," *SM Report No. 117*, University of Kansas Center for Research, Inc., 2016, 334 pp.
16. Hwang, H. J.; Park, H. G.; and Yi, W. J., "Nonuniform Bond Stress Distribution Model for Evaluation of Bar Development Length," *ACI Structural Journal*, V. 114, No. 4, July-Aug. 2017, pp. 839-849. doi: 10.14359/51689446
17. Hwang, H. J.; Park, H. G.; and Yi, W. J., "Development Length of Standard Hooked Bar Based on Nonuniform Bond Stress Distribution," *ACI Structural Journal*, V. 114, No. 6, Nov.-Dec. 2017, pp. 1637-1648. doi: 10.14359/51700918
18. ASTM A970/A970M-15, "Standard Specification for Headed Steel Bars for Concrete Reinforcement," ASTM International, West Conshohocken, PA, 2015, 9 pp.
19. Eligehausen, R.; Popov, E. P.; and Bertero, V. V., "Local Bond Stress-Slip Relationships of Deformed Bars under Generalized Excitations," *Earthquake Engineering Research Council Report No. 82/23*, University of California, Berkeley, Berkeley, CA, 1983, 169 pp.
20. Viwathanatepa, S.; Popov, E. P.; and Bertero, V. V., "Effects of Generalized Loadings on Bond of Reinforcing Bars Embedded in Confined Concrete Blocks," *Earthquake Engineering Research Council Report No. 79/22*, University of California, Berkeley, Berkeley, CA, 1979, 304 pp.
21. Joint ACI-ASCE Committee 408, "Bond and Development of Straight Reinforcing Bars in Tension (ACI 408R-03)," American Concrete Institute, Farmington Hills, MI, 2003, 49 pp.

APPENDIX A: RATIO OF UNDAMAGED LENGTH TO OVERALL DEVELOPMNET LENGTH

To simplify the proposed method, undamaged length $l_1 + l_2 = 0.75l_d$ was assumed. To determine the simplified value, a parametric study was performed. The results are summarized in **Fig. A1**. As shown in the figure, the ratio of the test strength to prediction show the lowest, and the COV variance is also low. This indicates that the use of $l_1 + l_2 = 0.75l_d$ results in the high accuracy of the prediction. This result was also reported in the previous studies.^{16,17} However, for better prediction, independent lengths of l_1 and l_2 satisfying **Eq. (11)** needs to be used in **Eq. (16)**.

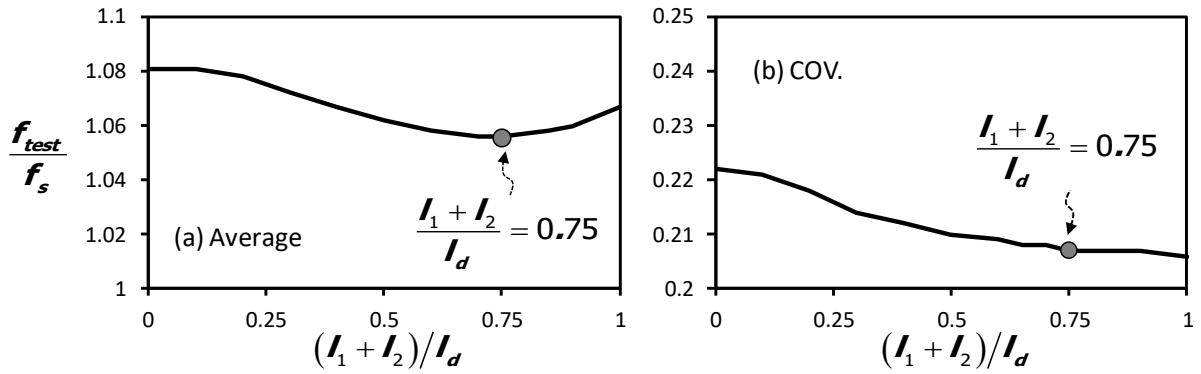


**Fig. A1 - Headed bar stress ratio of all test specimens according to the ratio of
undamaged length to development length**

APPENDIX B: DESIGN PARAMETERS OF PROPOSED MODEL

Table B1 lists the values of the design parameters. For given design parameters, three bond stresses and bearing stress of the head are calculated in sequence from the top to bottom. When each parameter is between two values, interpolation can be used (e.g. from $(cw + K_{atr})/d_b = 1.5$, $\tau_u/(\alpha_d \sqrt{f'_c}) = (0.364 + 0.725)/2$).

Table B1 Design parameters of proposed model [1 in = 25.4 mm; 1 ksi = 6.90 MPa]

Equations	Calculations					
$\tau_u = 0.91\alpha_d \sqrt{f'_c} \left[\frac{(c_0 w + K_{atr})/d_b}{2.5} \right]$ <p>for lap splice</p>	$(cw + K_{atr})/d_b$	1	2	3	4	5
	$\tau_u/(\alpha_d \sqrt{f'_c})$	0.364	0.725	1.092	1.456	1.456
$\tau_u = \frac{0.91\alpha_d \sqrt{f'_c}}{\alpha_{m1}\alpha_{m2}\alpha_{m3}}$ <p>for CCT node and beam-column joint</p>	$\alpha_{m1}\alpha_{m2}\alpha_{m3}$	0.6	0.7	0.8	0.9	1.0
	$\tau_u/(\alpha_d \sqrt{f'_c})$	1.517	1.300	1.138	1.011	0.910
$\frac{s_{l1}}{s_1} = \frac{F_h d_h}{257 f'_c} \left(\frac{1}{A_{nh}/A_b} \right) \leq 1$	Use F_h and A_{nh} of head					
$\tau_1 = \tau_u \left(\frac{s_{l1}}{s_1} \right)^{0.4}$	s_{l1}/s_1	0.0	0.25	0.5	0.75	1.0
	τ_1/τ_u	0.0	0.574	0.758	0.891	1.0
$\tau_2 = \frac{\tau_u}{1.4} \left[\frac{1 - (s_{l1}/s_1)^{1.4}}{1 - (s_{l1}/s_1)} \right] \leq \tau_u$	s_{l1}/s_1	0.0	0.25	0.5	0.75	1.0
	τ_2/τ_u	0.714	0.816	0.887	0.947	1.0
$C_1 = \frac{l_d}{4(1 - \sqrt{0.003 f'_c}) E_s d_b}$	l_d/d_b	5	10	15	20	25
	C_1 for $f'_c = 20$ MPa	8.28E-6	1.66E-5	2.48E-5	3.31E-5	4.14E-5
	C_1 for $f'_c = 40$ MPa	9.56E-6	1.91E-5	2.87E-5	3.83E-5	4.78E-5
	C_1 for $f'_c = 60$ MPa	1.09E-5	2.17E-5	3.26E-5	4.34E-5	5.43E-5
$\tau_3 = \left[\frac{4 - C_1 \{8d_h(\tau_1 - \tau_2) + 6l_d\tau_2\}}{4 + C_1 l_d \tau_u} \right] \tau_u$ $\geq \frac{\tau_u}{2}$	$C_1 l_d \tau_u$	0.01	0.05	0.1	0.3	0.5
	τ_3/τ_u for $s_{l1}/s_1 = 0.0$	0.99- 0.01 d_h/l_d	0.93- 0.07 d_h/l_d	0.87- 0.14 d_h/l_d	0.63- 0.40 d_h/l_d	0.500
	τ_3/τ_u for $s_{l1}/s_1 = 0.5$	0.98	0.92- 0.01 d_h/l_d	0.85- 0.03 d_h/l_d	0.56- 0.07 d_h/l_d	0.500
	τ_3/τ_u for $s_{l1}/s_1 = 1.0$	0.983	0.914	0.829	0.512	0.500
$F_h = \psi \frac{A_{Nc} \sqrt{f'_c}}{0.72 n A_b \sqrt{l_d}} \left(0.7 + \frac{c}{5l_d} \right)$	Use ψ and A_{Nc}					
$f_s = \frac{l_d}{d_b} \left[(\tau_1 - \tau_2) \frac{4d_h}{l_d} + 3\tau_2 + \tau_3 \right] + F_h \leq f_y$	Use τ_1 , τ_2 , and τ_3					

* α_d is coefficient related to rebar diameter (= 1.1 for D19 bars or less, 1.0 for D22 to D29 bars, and 0.9 for D32 bars or greater; $c_0 w + K_{atr}$ is coefficient-related transverse bars specified in ACI 408R-03; $\alpha_{m1}\alpha_{m2}\alpha_{m3}$ is coefficient related to concrete cover and transverse reinforcement; d_b is reinforcing bar diameter; d_h is head diameter; f'_c is concrete compressive strength; A_b is cross-sectional area of reinforcing bar; A_{nh} is net head area; l_d is development length; E_s : elastic modulus of reinforcing bar (= 200000 MPa); c is minimum cover dimension measured from bar center; ψ is strength increment factor; A_{Nc} is projected concrete failure area; n is the number of headed bars; and f_y is reinforcing bar yield strength.

APPENDIX C: TEST PARAMETERS AND COMPARSION BETWEEN TEST RESULTS AND PREDICTIONS

Tables C1 and C2 list the principal test parameters and comparison between test results and predictions of 50 existing CCT node test specimens, 40 existing lap splice test specimens, and 271 existing beam-column joint test specimens^{3,5,8,9,12-15}, respectively.

Table C1 Test parameters of existing test specimens [1 in = 25.4 mm; 1 ksi = 6.90 MPa]

Specimens	Number of tests	Types	l_d (mm)	d_b (mm)	f'_c (MPa)	f_y (MPa)	Coefficients
Thompson et al. ⁸	40	CCT node	254-635	25.4-36.0	21.0-28.0	433-472	0.60-0.72
Shao et al. ¹⁵	10	CCT node	229-356	25.4	31.0-39.7	890	0.72
Thompson et al. ⁹	10	Lap splice	203-356	25.4	24.0-29.0	472	2.53-4.00
Chun et al. ¹²	24	Lap splice	429-858	25.4-28.6	20.3-62.9	601-710	1.45-4.00
Shao et al. ¹⁵	6	Lap splice	305	19.1	43.7-75.1	826	2.24-3.17
Bashandy ³	18	Joint	204-432	25.4-35.8	22.1-39.6	556-578	0.76-0.84
Choi et al. ⁵	4	Joint	190	19.1	27.1	506	0.60
Sim et al. ¹⁴	20	Joint	89-191	22.2-31.8	130-226	649-679	0.73-0.85
Chun et al. ¹³	27	Joint	301-917	43.0-57.3	40.5-81.2	583-606	0.70-1.00
Shao et al. ¹⁵	202	Joint	97-499	15.9-35.8	27.3-111	799-959	0.60-0.85
Total	361	-	89-917	15.9-57.3	20.3-226	433-959	0.60-4.00

* l_d : development length; d_b : reinforcing bar diameter; f'_c : concrete compressive strength; f_y : reinforcing bar yield strength; and Coefficients: $(cw+K_{atr})/d_b$ for lap splice; and $\alpha_{m1}\alpha_{m2}\alpha_{m3}$ for CCT node and beam-column joint.

Table C2 Comparison between test results and predictions

Specimens	f_{test}/f_s (ACI 318-14)	f_{test}/f_s (MC 2010)	f_{test}/f_s (Thompson model)	f_{test}/f_s (Shao model)	f_{test}/f_s (Proposed Eq. (21))	f_{test}/f_s (Proposed Eq. (22))
Thompson et al. ⁸	2.27 ± 0.23	1.81 ± 0.19	1.13 ± 0.22	1.68 ± 0.50	1.27 ± 0.17	1.43 ± 0.19
Shao et al. ¹⁵	2.33 ± 0.35	3.49 ± 0.51	1.70 ± 0.27	1.78 ± 0.32	1.33 ± 0.23	1.35 ± 0.27
Thompson et al. ⁹	1.80 ± 0.42	1.29 ± 0.21	1.19 ± 0.17	1.09 ± 0.17	0.93 ± 0.12	1.01 ± 0.14
Chun et al. ¹²	0.66 ± 0.18	1.81 ± 0.23	1.17 ± 0.31	0.97 ± 0.15	1.12 ± 0.12	1.14 ± 0.13
Shao et al. ¹⁵	0.94 ± 0.12	2.73 ± 0.63	1.02 ± 0.26	1.40 ± 0.14	0.84 ± 0.11	0.88 ± 0.12
Bashandy ³	1.52 ± 0.25	1.83 ± 0.35	1.13 ± 0.25	1.74 ± 0.36	1.25 ± 0.25	1.32 ± 0.26
Choi et al. ⁵	1.86 ± 0.04	1.17 ± 0.03	1.40 ± 0.03	1.23 ± 0.03	0.99 ± 0.01	1.02 ± 0.02
Sim et al. ¹⁴	2.67 ± 0.40	2.04 ± 0.34	0.75 ± 0.13	2.97 ± 0.48	1.02 ± 0.04	1.03 ± 0.05
Chun et al. ¹³	1.20 ± 0.21	2.00 ± 0.36	1.17 ± 0.25	1.43 ± 0.28	1.20 ± 0.18	1.26 ± 0.19
Shao et al. ¹⁵	1.64 ± 0.57	1.82 ± 0.49	0.81 ± 0.33	1.27 ± 0.26	0.97 ± 0.19	1.00 ± 0.20
Min. to Max.	0.44-3.90	0.87-4.19	0.24-2.28	0.70-3.77	0.48-1.71	0.50-1.81
Average + SD.	1.68 ± 0.65	1.88 ± 0.53	0.95 ± 0.36	1.43 ± 0.53	1.06 ± 0.22	1.10 ± 0.25
COV.	0.386	0.282	0.379	0.366	0.207	0.225

Reproduced with permission of copyright owner. Further reproduction
prohibited without permission.